Ultrasonic Attenuation Coefficient Estimate of Placenta is correlated to MRI Proton-Density-Fat Fraction: A Preliminary *Ex Vivo* Study

Farah Deeba*, Caitlin Schneider*, Ricky Hu*, Victoria Lessoway‖, Jefferson Terry†, Denise Pugash‡, Jennifer A. Hutcheon§, Chantal Mayer§ and Robert Rohling*¶
*Department of Electrical and Computer Engineering, University of British Columbia, Vancouver, British Columbia, Canada
‖Department of Ultrasound, BC Women's Hospital, Vancouver, Canada
†Department of Pathology and Laboratory Medicine, University of British Columbia, Vancouver, British Columbia, Canada
‡Department of Radiology, University of British Columbia, Vancouver, British Columbia, Canada
§Department of Obstetrics and Gynaecology, University of British Columbia, Vancouver, British Columbia, Canada
¶Department of Mechanical Engineering, University of British Columbia, Vancouver, British Columbia, Canada
Email: {rohling, farahdeeba}@ece.ubc.ca

2021 IEEE International Ultrasonics Symposium (IUS) | 978-1-6654-0355-9/21/$31.00 ©2021 IEEE | DOI: 10.1109/IUS52206.2021.9593905

***Abstract*—This work explores a non-invasive imaging approach for quantifying placental fat. First, we show the efficacy of MRI proton-density-fat-fraction (PDFF) to accurately measure fat percentage in a phantom study. We found that ultrasonic attenuation coefficient estimate (ACE) is strongly correlated to the MRI PDFF in the phantoms. In the *ex vivo* placental study, we demonstrate that the spatial variation in MRI PDFF map and ultrasonic ACE map are correlated.**

***Index Terms*—Attenuation Coefficient Estimate, proton-density-fat-fraction, placenta**

I. Introduction

The association of ultrasonic attenuation coefficient estimate (ACE) and MRI Proton-Density-Fat-Fraction (PDFF) has been widely researched in relation with the presence of fat in hepatic cells [1]–[3]. While MRI PDFF is the current gold standard to quantify the fat content in hepatic cells [2], it is not feasible for routine screening due to its prohibitive cost. On the other hand, ultrasonic ACE provides an indirect measure of fat. Fat droplets in the fatty liver cause cellular ballooning, which affects the ultrasonic scattering process, resulting in an increase in ACE. With a strong correlation to MRI PDFF, ACE is being recognized as a more accessible alternative to MRI PDFF for fatty liver disease detection [1]–[3].

The form, type and size of fatty acid molecules deposited in the placenta, the underlying mechanisms and the implications are very different and also relatively less studied compared to the fat contents in liver. The placenta, being the primary facilitator for the transfer of nutrients from mother to fetus, regulates the availability of fatty acids, adapting to constant changes in demands for the developing fetus as well as for itself [5]. Recent research found that placentas from pregnancies complicated with preeclampsia had significantly higher lipid content than healthy placentas (40% higher triacyglycerol and 33% higher cholesteryl ester) [6]. Hypoxia, which refers to the insufficient utero-placental oxygenation, is a key component of placental dysfunction, and is associated with intra-uterine growth restriction and preeclampsia. It was showed that placental tissue cultured in hypoxic environment deposit lipids in the form of lipid droplet [5]. A separate study hypothesized that the increase in lipid trapping occurs into the placenta due to reduced utilization, rather than the increased storage [7]. Therefore, increased lipid storage in the placenta could be an indicator of inefficient lipid transport to the fetus, altered placental energy storage and utilization, or protection against lipotoxicity.

Fat in the placenta accumulate as droplets with size ranging between 1-100 micrometer in the endoplasmic reticulum. Fat in the placenta requires powerful optical modalities, such as fluorescent microscope and exogenous absorbers to label lipid droplets for visualization [5]. Optical imaging, while providing sub-atomic resolution, is limited by low penetration depth. The need for exogenous agents further limits the application of most optical modalities to *in vitro* and *ex vivo* specimens. There is an unmet need to identify appropriate imaging modalities that do not require exogenous labels and can attain sufficient penetration depth for the visualization of placental fat deposition *in vivo*. Based on our previous *in vivo* liver study, we propose two modalities namely MRI-PDFF and ultrasonic ACE for non-invasive *in vivo* imaging of the placental fat. Previosuly, only the ultrasonic ACE of normal placentas have been studied [8], while the role of ACE in placental abnormality detection is yet to be established. In the current work, we collect ultrasound ACE and MRI PDFF data from placenta *ex vivo* from both normal and diseased placentas. We also acquire histopathology data. We designed and applied an data acquisition and alignment protocol to register images from these different modalities. From the registered dataset, we investigate the spatial variation of fat in the placenta with MRI-PDFF and ultrasound ACE. Additionally, we analyze the correlation between these two parameters using phantom and *ex vivo* placentas. We also investigate the spatial variation of ACE and PDFF measures in focal lesions, namely

978-0-7381-1209-1/21/$31.00 ©2021 IEEE

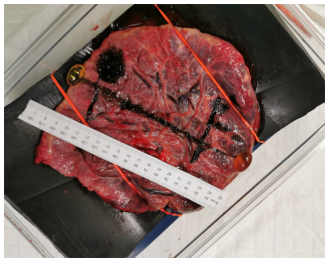

Fig. 1: Digital photograph showing the placenta marking using India ink and cod liver oil.

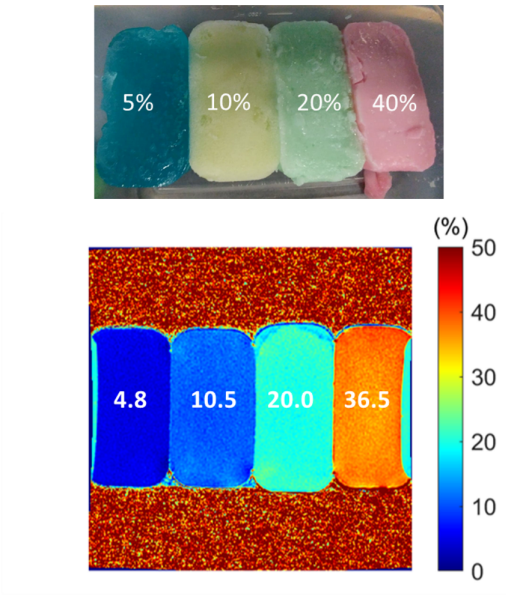

Fig. 2: Set of 4 phantoms with the actual fat percentage annotated (top) and the MRI proton-density-fat-fraction (PDFF) map (bottom).

chorangioma for an example case.

II. Method

A. Data

In this study, 46 placentas were collected from a group of women who delivered via cesarean delivery at BC Women's Hospital, Vancouver, Canada. The study (H17-00331) was performed under written informed consent of all participants after approval by the University of British Columbia Children's and Women's Research Ethics Board. We included 24 placentas from pregnancies affected by PE and/or IUGR and 22 placentas from healthy pregnancies. For validation, a set of 4 oil-in-gelatin phantoms were manufactured with 5%, 10%, 20% and 40% fat (oil) by weight [9].

B. Placenta Preparation and Marking

The placentas were stored at 4°C until the examination. Before examination, layers of acoustic absorbing pad (Aptflex F28, Precision Acoustics, UK) were placed beneath the maternal surface of the placenta disc to reduce reverberation artifacts. The placenta was secured using two rubber bands at the edges to the absorbing pad layers and then placed in a rigid plastic container to minimize any deformation while transporting from one imaging modality to another. A sonographer (V.L.) scanned the placenta to locate two regions-of-interest, such that both regions lie on the same axial-lateral plane. India ink was applied to mark the identified regions and the corresponding plane-of-interest on the fetal surface of the placenta. Two cod liver oil pills (considered as MRI visible fiducials) were then placed at the edges of the placenta along the in-plane line. An example of placenta preparation and marking has been shown in figure 1.

C. Magnetic Resonance Imaging

The MRI protocol was reviewed and approved by the BC Children's Hospital (BCCH) MRI Research Facility's Protocol Review Committee. MRI scans were performed on a GE Discovery MR750 3.0T MRI scanner (GE Healthcare, Milwaukee, Wisconsin) using an 8-channel cardiac array. The placenta was positioned such that the laser beam localizer aligns to the mark on the fetal surface indicating the plane-of-interest. Three-plane-localiser using a standard spin-echo pulse sequences were first performed to visualize the overall structure of the placenta and to facilitate the subsequent acquisitions. MR PDFF imaging was performed on 40 placentas using a T2-weighted fast-spin-echo FLEX sequence, resulting in fat-only (F) and water-only (W) images. Fat fraction was computed from these two images using the following equation: $PDFF = \frac{F}{W+F} \times 100\%$.

D. Quantitative Ultrasound

Volumetric ultrasound radio-frequency data were acquired using Ultrasonix SonixTouch ultrasound machine (Analogic, Richmond, BC, Canada), with a m4DC7-3/40 curved array transducer (Ultrasonix, Richmond, BC, Canada). To compute ACE, the data acquired from the tissue were normalized by the data from a well-characterized reference phantom, manufactured by CIRS (Northfolk, VA, USA), acquired using the same transducer and system settings. With a piece-wise continuous assumption in all the three directions, we apply a 3D total variation regularization approach to reconstruct ACE maps [4].

E. Histopathology

After imaging, each placenta underwent pathological examination. The placenta was sampled in such a way that the full-thickness sections included the volumes of interest acquired during ultrasound and MRI. After routine formalin fixation, processing, and hematoxylin and eosin staining, the slides were scanned with the Aperio ScanScope system (Aperio, Vista, CA). The pathologic slides were reviewed by an experienced perinatal pathologist (J.T.) .

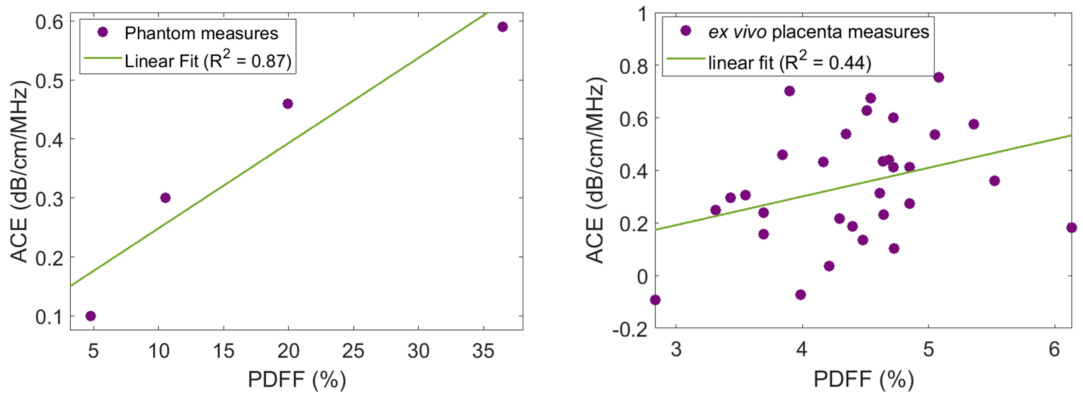

Fig. 3: Ultrasonic ACE versus MRI PDFF for phantom (left) and ACE versus PDFF for *ex vivo* placental tissue.

F. Registration

The image acquisition protocol described above ensures that the center plane in the ultrasound, MRI and pathology image volumes are aligned. While MR imaging includes the entire axial plane, the ultrasound and pathology images include sections of the planes centring around the marked locations. To identify the placenta locations in MRI corresponding to the ultrasound and pathology, we perform the registration between the MRI and the digital photograph of the fetal surface along with the marking and MRI-visible fiducials. First, we identify the coronal slice in the MR localiser sequence images, that contains the fiducials. The co-ordinates of the fiducials in the reference MR image and the digital photograph were identified and registered using coherent point drift (CPD) algorithm, a rigid point-set registration method [10]. The digital photograph was registered to the MRI using a transformation matrix computed during the previous step. The MRI locations corresponding to the ultrasound and pathology are computed by measuring the distance between the fiducials and the ink marks in the registered digital photograph. The registration of the center plane in ultrasound and pathology volume to the MRI central plane are then fine-tuned using anatomic landmarks identifiable in all the modalities.

III. Results

The PDFF values obtained for the reference phantoms were 4.8%, 10.5%, 20.0% and 36.5%, respectively (figure 2). The obtained ACE measures were well-correlated to the reference MRI PDFF values ($R^2 = 0.87$), showing the reliability of ACE measures. The ACE and PDFF measures obtained for the *ex vivo* placentas were found to be moderately correlated ($R^2 = 0.44$). The correlation results have been shown in figure 3. We also study the ACE and PDFF measures observed in focal lesions, namely chorangioma and compare with those found in a homogeneous region without any lesion. With this objective, we first register the multimodal image data (figure 4 (left)). The ACE and PDFF maps both showed lower values in the chorangioma region compared to those in the normal region. The PDFF value in the lesion region was 1.8%, whereas the normal section was associated to a PDFF value of 5.4%. The ACE values in the lesion region and normal regions were 0.1 dB/cm/MHz and 0.41 dB/cm/MHz, respectively. These results have been shown in figure 4. The decrease in PDFF and ACE could be a result of relatively increased water content in the infarcted chorangioma.

IV. Conclusion

This is the first study to show the spatial variations of MRI PDFF and ultrasonic ACE for the placenta obtained from normal and diseased placentas. We also investigated the correlation of MRI PDFF and ultrasonic ACE for focal placental lesions using a single case study. This study unveils a new research avenue for the understanding of placental pathology using non-invasive imaging techniques. Further research is warranted to understand the complex relationship between the fat distribution and placenta-mediated disorders.

Acknowledgment

This work was supported by Microsoft corporation, Schlumberger foundation, Natural Sciences and Engineering Research Council of Canada (NSERC) and the Canadian Institutes of Health Research (CIHR). The authors would also like to thank BC Children's Hospital BioBank for the support in placenta sample collection.

References

[1] Paige, Jeremy S., et al. "A pilot comparative study of quantitative ultrasound, conventional ultrasound, and MRI for predicting histology-determined steatosis grade in adult non-alcoholic fatty liver disease," American Journal of Roentgenology 208.5, pp. W168–W177, 2017.

[2] Noureddin, M., et al. "Utility of magnetic resonance imaging versus histology for quantifying changes in liver fat in nonalcoholic fatty liver disease trials," Hepatology, 58(6), pp. 1930–1940, 2013.

[3] Deeba, F.,Schneider, C., Mohammed, S., Honarvar, M., Tam E., Salcudean, S., and Rohling, R., "SWTV-ACE: spatially weighted regularization based attenuation coefficient estimation method for hepatic steatosis detection," International Conference on Medical Image Computing and Computer-Assisted Intervention, pp. 610–618, Springer, Cham, 2019.

[4] Deeba, F.,Schneider, C., Mohammed, S., Honarvar, M., Lobo, J., Tam E., Salcudean, S., and Rohling, R., "A Multiparametric Volumetric Quantitative Ultrasound Imaging Technique for Soft Tissue Characterization." arXiv preprint arXiv:2104.00712, 2021.

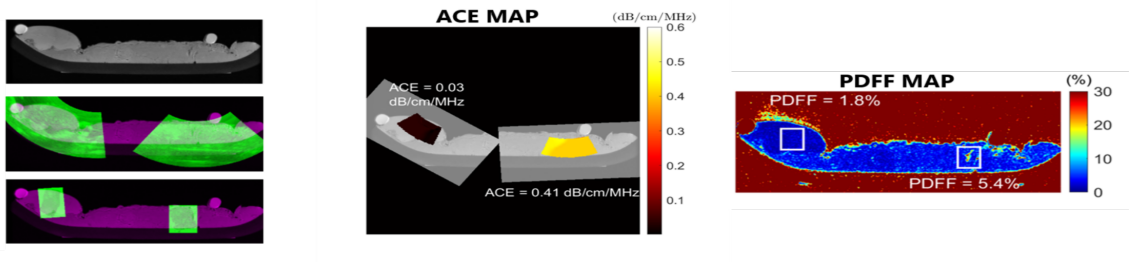

Fig. 4: Left: Multimodal registration for an example placenta case: MRI PDFF image (top), ultrasound overlaid on MRI (middle), and pathology images overlaid on MRI (bottom). Middle: Ace map overlaid on the MRI. The mean ACE value for two regions-of-interest have been shown. Right: PDFF map showing mean PDFF for the corresponding regions-of-interest.

[5] Scifres, C., and Sadovsky, Y., "Placental fat trafficking," The Placenta, pp. 75–80, 2011.

[6] Brown, Simon HJ, et al. "A lipidomic analysis of placenta in preeclampsia: evidence for lipid storage," Plos One 11.9, pp. e0163972, 2016.

[7] Louwagie, Eli J., et al. "Placental lipid processing in response to a maternal high-fat diet and diabetes in rats," Pediatric Research 83.3, pp. 712–722, 2018.

[8] Deeba, F., et al., "Attenuation coefficient estimation of normal placentas," Ultrasound in Medicine & Biology , pp. 29-31, 2019.

[9] Nguyen, Man M., et al. "Development of oil-in-gelatin phantoms for viscoelasticity measurement in ultrasound shear wave elastography," Ultrasound in Medicine & Biology 40.1, pp. 168–176, 2014.

[10] Myronenko, A., Song, X., "Point set registration: Coherent point drift. IEEE Transactions on Pattern Analysis and Machine Intelligence," 32, pp. 2262-2275, 2010.